

Integrating Active Learning in Causal Inference with Interference: A Novel Approach in Online Experiments

Hongtao Zhu
National University of Singapore
Singapore, Singapore, Singapore
hongtao.zhu@u.nus.edu

Sizhe Zhang
Tencent
Singapore, Singapore, Singapore

Yang Su
Tencent
Palo Alto, California, USA
yaangsu@global.tencent.com

Zhenyu Zhao
Tencent
Palo Alto, California, USA

Nan Chen
National University of Singapore
Singapore, Singapore, Singapore
isecn@nus.edu.sg

ABSTRACT

In the domain of causal inference research, the prevalent potential outcomes framework, notably the Rubin Causal Model (RCM), often overlooks individual interference and assumes independent treatment effects. This assumption, however, is frequently misaligned with the intricate realities of real-world scenarios, where interference is not merely a possibility but a common occurrence. Our research endeavors to address this discrepancy by focusing on the estimation of direct and spillover treatment effects under two assumptions: (1) network-based interference, where treatments on neighbors within connected networks affect one's outcomes, and (2) non-random treatment assignments influenced by confounders. To improve the efficiency of estimating potentially complex effects functions, we introduce a novel active learning approach: Active Learning in Causal Inference with Interference (ACI). This approach uses Gaussian process to flexibly model the direct and spillover treatment effects as a function of a continuous measure of neighbors' treatment assignment. The ACI framework sequentially identifies the experimental settings that demand further data. It further optimizes the treatment assignments under the network interference structure using genetic algorithms to achieve efficient learning outcome. By applying our method to simulation data and a Tencent game dataset, we demonstrate its feasibility in achieving accurate effects estimations with reduced data requirements. This ACI approach marks a significant advancement in the realm of data efficiency for causal inference, offering a robust and efficient alternative to traditional methodologies, particularly in scenarios characterized by complex interference patterns.

CCS CONCEPTS

• **Mathematics of computing** → **Probability and statistics**.

KEYWORDS

Causal inference, Network interference, Gaussian process regression, Active learning, Experimental design, Genetic optimization

1 INTRODUCTION

1.1 Motivation

In the realm of causal inference, observational studies have traditionally relied on regression-based and matching-based approaches to estimate treatment effects. They work with messy data and seek

to estimate treatment effects using regression models [6, 16, 20, 22] or matching methods [1, 2]. Most studies assumed the absence of interference between two individuals, meaning that one individual's information, including treatment, features, and outcomes, does not affect others. In reality, interference is prevalent. For example, one person's increased online gaming time may be influenced by their friends' participation in certain in-game activities. Studies in other domains, including but not limited to health [12, 13], education [11, 15, 36], social interactions [8], and politics [5] have shown interference affects treatment effects. Clearly, considering interference in causal inference is a highly practical and relevant topic.

1.2 Related work

Presently, numerous studies within the field of causal inference aim to estimate treatment effects through experimental or non-experimental approaches. The majority of these investigations are grounded in the potential outcomes framework [7, 29], commonly referred to as the Rubin Causal Model (RCM), which is underpinned by three core assumptions: Stable Unit Treatment Value Assumption (SUTVA) [30], Exchangeability Assumption and Positivity Assumption [14, 28]. Based on this framework, numerous methodologies for effect estimation in causal inference have been developed [1, 2, 6, 20, 26, 38]. Notably, all the methods discussed earlier are based on the assumption of no interference (SUTVA), which posits that one individual's information, including treatment, features, and outcomes, does not affect others. However, interference is a common occurrence in the real world, where one individual's actions or treatment can impact others' outcomes. This real-world interference adds complexity to causal inference and often necessitates the use of advanced statistical and modeling techniques.

Recently, the number of papers addressing causal inference with interference or estimating treatment effects in the presence of interference has grown significantly. There is a growing emphasis on estimating two distinct effects: the direct treatment effect, which refers to the impact of an individual's own treatment on their outcome, and the spillover effect, alternatively termed the indirect treatment effect, which pertains to the influence of treatments assigned to an individual's neighbors on the individual's outcome [17].

Current methods for causal inference in the presence of interference can be broadly categorized into two main groups: randomized

experiments and observational studies. Randomized experiments methods employ specific randomization techniques, such as cluster randomization or network randomization [3–5, 8, 17, 27, 33]. Early methods were developed to estimate the overall treatment effects in the presence of interference, which is the sum of both the direct treatment effects and the spillover effects [27]. A two-stage randomization procedure has been proposed to facilitate the estimation of direct treatment effects and spillover effects separately within clusters [17]. There have also been refinements in controlling the variance of treatment effects to obtain better Horvitz–Thompson type estimators [3]. Additionally, complex scenarios have been introduced, for example, [8] uses Encouragement Designs to explore the endogenous behavior of interest. However, these methods cannot be applied in observational studies or in specific experiments where proper randomization is not feasible.

In terms of observational studies, some research focuses on the intricacies of causal and network structures, providing direction and theoretical foundation for the further estimation of treatment effects. Notably, studies utilizing Directed Acyclic Graphs (DAGs) have been instrumental in elucidating the causal structure in the presence of interference. For example, works by Ogburn and Sherman present a potential outcomes framework under interference, revealing the intricate structure of interference and guiding further statistical analysis [24, 32]. The following Figure 1, as illustrated in [24], displays the causal structure in the scenario where interference is present. With a clear definition of causal structure and effects, several methodologies [9, 10, 19, 21, 23, 34, 35] have been developed to effectively estimate potential outcomes or effects under various treatment levels.

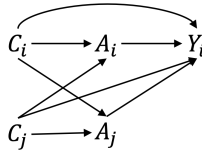


Figure 1: Illustrative causal structure of individual i interfering with individual j .

The use of Inverse Probability Weighting (IPW) methods has also been extended to address network inference [21, 34]. [21] build upon the work of [34] to introduce a robust IPW estimator to estimate effects based on clusters. However, similar to traditional IPW estimation, this method heavily relies on correct specification of propensity score functions and assumes treatment assignments through Bernoulli allocation strategies. It could lead to significant biases in treatment effect estimation if the model structure of the propensity score functions is misspecified.

Another branch of methodologies has been developed focusing on network-based approaches (a network example is shown in Figure 2). These include the Targeted Maximum Likelihood Estimator (TMLE) [23, 35], methods within the Bayesian framework [9, 10], and applications of Graph Neural Networks (GNNs) [19].

The Targeted Maximum Likelihood Estimator (TMLE), as proposed in [35], has been utilized in observational studies within networks to estimate average potential outcomes in the presence of interference [23]. In their research, [23] employed an approach that

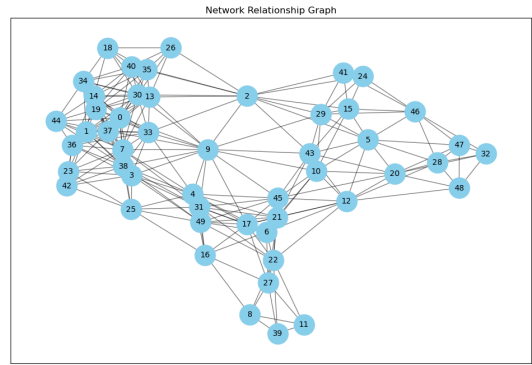


Figure 2: The social network of 50 individuals.

integrates the covariates and treatments of neighbors. However, TMLE remains a parametric method, relying on correct model specification. Its primary objective is to estimate the average potential outcome under a determined treatment assignment strategy, which differs from the focus of our research.

The Bayesian framework has been applied to address interference, allowing for more flexible modeling assumptions and complex model structures [9, 10]. This approach is also network-based and involves integrating information from neighbors. The estimand in their work aligns with ours, focusing on average effect functions with the integrated treatment level as input. However, a significant challenge arises due to the "Curse of Dimensionality" in the context of high-dimensional covariates. Sparse data in such scenarios tend to skew results towards the prior, impacting the robustness and reliability of the outcomes.

Machine learning techniques, such as deep learning, are also employed to estimate interference effects. Graph Neural Networks (GNNs) have been proposed as a potential solution to the causal inference with interference problem [19]. A key advantage of GNNs is their ability to circumvent the loss of information often encountered when integrating neighbors' data. However, it is worth noting that GNNs underperform when dealing with overly complex social networks.

In summary, current observational studies in causal inference with interference fall short in effectively addressing the challenges in estimating treatment effects. The most common issue is they rely on correct parametric model assumptions, making it difficult to adapt to the complex real-world problems.

1.3 Contributions

In this paper, we consider the estimation of direct treatment effects and spillover effects when network-based interference is present in online experiments. Instead of relying on parametric model specification, we propose a nonparametric method based on Gaussian process (GP) to quantify the effects at different degree of the interference.

GP is a flexible regression model that can approximate a wide range of functional relationships. In addition, GP provides uncertainty quantification and points out the areas that require more samples to improve the approximation accuracy. This feature makes

it particularly useful in online experiments, where sequential experimental designs are relatively easier to conduct. Hinging on this feature, we propose an active learning strategy for designing and analyzing online experiments. Unlike experiments without interference, where the treatment assignment can be precisely conducted, the degree of interference can hardly be controlled precisely in networks. Therefore, even with active learning in choosing the experimental design, we still need to integrate methods from observational studies to utilize all samples best.

In our proposed framework, we use GP to model the potential outcomes of each individual, given the treatment and covariates of the individual and its neighbors. Because of the varying network structure, the number of neighbors or the degree of interference can be different. We use active learning to determine the design of new experiments so that we can have data at desired interference levels. This iterative process continues until the budget runs out or the effects have been estimated with sufficient accuracy. The diagram of the iterative process is illustrated in Figure 3.

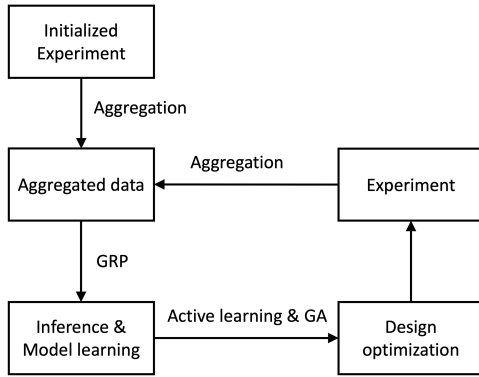


Figure 3: The structure of our active learning framework designed for causal inference with interference (GA: Genetic algorithm, GRP: Gaussian process regression). A detailed exposition of this framework is provided in Section 3.

In summary, our work’s contributions include: (1) We introduce active learning to causal inference with interference, by which we dynamically select the most informative data points to enhance efficiency and accuracy in effect estimation. (2) We employ a non-parametric method for effect estimation, which is resistant to model misspecification and adept at capturing non-linear relationships. (3) We proposed a genetic algorithm to optimize the treatment assignments to have the desired level of network interference.

The remainder of this article is organized as follows. Section 2 presents the model formulation and introduces the potential outcomes framework that takes into account network-based interference. Section 3 discuss in details our methodology, including GP modeling, active learning strategy, and treatment assignment optimization. Section 4 demonstrates the performance of the method through simulations and an empirical study using a real dataset. Section 5 concludes the paper with discussions.

2 PRELIMINARIES AND PROBLEM FORMULATION

In this section, we outline the key assumptions relevant to our study and provide a comprehensive methodology for integrating covariates and treatments.

2.1 Network assumption

To represent networks for all n individuals, we utilize a relationship matrix denoted as $W \in \mathbb{R}^{n \times n}$. In this matrix, vector W_i represents the relationships of individual i with all its neighbors, and element w_{ij} indicates the strength of the relationship between two individuals, i and j . When i and j are not neighbors—implying no connection such as in-game friends—the value w_{ij} is set to 0. In contrast, if i and j are neighbors, w_{ij} is assigned a positive real number reflecting the strength of their relationship. As a special case, $W \in \mathbb{R}^{n \times n}$ takes binary values, with $w_{ij} = 1$ denoting the existence of the relationship between i and j , and 0 otherwise. Figure 4 displays a sub-network of the network presented in Figure 2 for individual 1. This sub-network includes individual 1 and all its neighbors, with individual 1 defined as the central node of this specific sub-network.

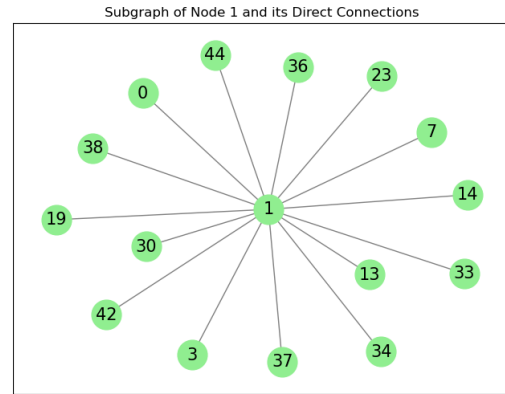


Figure 4: Illustrative Sub-Network Centered Around Individual 1, where connections indicate relationships between individuals, e.g., $w_{1,0} = 1$.

2.2 Potential outcomes framework with interference

Building upon [29] and [24], we define our potential outcomes framework with interference as follows. In our notation, we employ Y to denote the outcome, A to represent a binary treatment, i.e., $A = 0$ or 1 , and C to represent confounders with dimension p . An individual i is completely characterized by $\{Y_i, A_i, C_i\}$.

We denote the number of neighbors of individual i as m_i , and neighbors of individual i belongs to the collection $N_i^f = \{j \mid w_{ij} > 0\}$. For notation simplicity, we group the data for all m_i neighbors as $Y_i^N = [Y_j \mid j \in N_i^f] \in \mathbb{R}^{m_i}$, $A_i^N = [A_j \mid j \in N_i^f] \in \mathbb{R}^{m_i}$, $C_i^N = [C_j \mid j \in N_i^f] \in \mathbb{R}^{m_i \times p}$. Throughout this article, we use

uppercase letters to indicate random variables, and lowercase letters to indicate a realization, unless otherwise specified.

Each central individual often possesses its unique neighbor structures. For instance, the number of neighbors for individual i might differ from that of individual j . Consequently, the treatments (a_i, a_i^N) and (a_j, a_j^N) may have distinct dimensions and levels. To tackle this issue, a transformation function g_i is introduced:

$$G_i = g_i(A_i^N, W_i) \quad (1)$$

Here, G_i can represent the proportion of neighbors who have been subject to the treatment, or equivalently, the proportion of 1 within A_i^N . This approximation is similar to the one used by [9, 10].

It is essential to acknowledge that varying network structures can lead to differences in the sizes of C_i^N and C_j^N . Furthermore, the size of C_i^N can become considerably large, given the substantial number of neighbors. Considering that individuals receiving different treatments in observational studies are likely to have different distributions in covariates, we aim to control the transformed neighbor covariates within the same and reasonable size while minimizing information loss during the approximation process. To clarify further, our objective is to approximate neighbor covariates in a manner that retains, to a certain extent, their distribution information within specific A_i^N conditions. To achieve this, we introduce a transformation function h_i :

$$\tilde{C}_i^N = h_i(C_i^N, A_i^N, W_i) \quad (2)$$

For example, \tilde{C}_i^N could represent the average of C_i^N , i.e.,

$$\tilde{C}_i^N = \frac{\sum_{j=1}^{m_i} C_{i,j}^N}{m_i},$$

where m_i can be any natural number ($m_i \in \mathbb{N}$), accounting for the variable number of neighbors among central individual i . Of course, other reasonable choices of g_i, h_i functions can be used.

Considering the neighbors' information, an individual i can be characterized by $\{Y_i, (A_i, G_i), X_i\}$ where $X_i = (C_i, \tilde{C}_i^N)$. The three causal assumptions from section 2.2 can be expressed as follows:

- Assumption of consistency under interference:

$$Y_i(a, g) = Y_i \quad \text{when} \quad (A_i, G_i) = (a, g) \quad (3)$$

- Exchangeability assumption:

$$Y_i(a, g) \perp\!\!\!\perp (A_i, G_i) \mid X_i \quad (4)$$

- Positivity assumption:

$$P((A_i, G_i) = (a, g) \mid X_i) > 0 \quad (5)$$

2.3 Causal estimands

When considering the treatment (a, g) and the controlled level $(0, 0)$, we define an individual's overall treatment effect (represented as IOTE $_i$), direct treatment effect (represented as IDTE $_i$) and spillover effect (depicted as ISE $_i$) as follows:

$$\text{IOTE}_i(g) = \mathbb{E}[Y(1, g)|X_i] - \mathbb{E}[Y(0, 0)|X_i]$$

$$\text{IDTE}_i(g) = \mathbb{E}[Y(1, g)|X_i] - \mathbb{E}[Y(0, g)|X_i]$$

$$\text{ISE}_i(g) = \mathbb{E}[Y(0, g)|X_i] - \mathbb{E}[Y(0, 0)|X_i]$$

Similarly, we provide average level effects as follows, with average overall treatment effect τ_1 , average direct treatment effect $\tau_{1,0}$ and average spillover effect τ_0 :

$$\tau_1(g) = \mathbb{E}[\mathbb{E}[Y(1, g)|X] - \mathbb{E}[Y(0, 0)|X]]$$

$$\tau_{1,0}(g) = \mathbb{E}[\mathbb{E}[Y(1, g)|X] - \mathbb{E}[Y(0, g)|X]]$$

$$\tau_0(g) = \mathbb{E}[\mathbb{E}[Y(0, g)|X] - \mathbb{E}[Y(0, 0)|X]]$$

3 PROPOSED METHOD

We divide our proposed method into two parts. First, we use a method based on Gaussian process regression to estimate potential outcomes, thereby estimating individual treatment effects and average treatment effects. Second, we use active learning to identify how to assign new samples so that the treatment effects can be better estimated.

3.1 Gaussian Process Regression for Treatment Effects

Our proposed approach employs Gaussian Process Regression (GPR) to assess the treatment effects on the entire population at a specific treatment level $A = a$ and $G = g$. Specifically, we model the potential outcome as at treatment level a as $f_a(g, X)$. This methodology leverages all available observational data, especially outcomes from experimental settings, when the condition $A = a$ is met. We aim to forecast the potential outcomes for the whole population under the treatment level $A = a$ and $G = g$.

To implement Gaussian Process regression, we define our kernel function as $k((x, g), (x', g'))$. For more detailed examples of this kernel function, refer to the Appendix A.1. Consider a training dataset for a specific treatment $A = a$, with size n_t . This dataset comprises integrated covariates $\mathbf{X}_t = (X_{t,1}, \dots, X_{t,n_t})^T$, integrated neighbors' treatments $\mathbf{g}_t = (g_{t,1}, \dots, g_{t,n_t})^T$, and their actual outcomes $\mathbf{y}_t = (y_{t,1}, \dots, y_{t,n_t})^T$. By following the maximum likelihood framework, we can estimate the hyper-parameters to maximize the marginal (log) likelihood of the training data, as shown in Appendix A.2. Our goal is to predict the potential outcomes for the entire population, which includes a total of n individuals with integrated covariates $\mathbf{X} = (X_1, \dots, X_n)^T$, under the treatment level $A = a, G = g$. The predicted outcome function values are denoted as $\mathbf{f}_a(g, \mathbf{X}) = [f_a(g, X_1), \dots, f_a(g, X_n)]^T$.

To estimate the average treatment effects, we should determine the average potential outcome function $m_a(g)$ for the entire population under the treatment level $(A = a, G = g)$. This function is expressed as follows:

$$m_a(g) = \mathbb{E}_X[f_a(g, X)] = \int f_a(g, X) d\mathbb{P}(X), \quad (6)$$

which can be estimated by:

$$\hat{m}_a(g) = \frac{1}{n} \sum_{i=1}^n f_a(g, X_i) = \frac{1}{n} \mathbf{e}^T \cdot \mathbf{f}_a(g, \mathbf{X}), \quad (7)$$

where $\mathbf{e} = (1, \dots, 1)^T$ with length n .

We represent the kernel matrix used in our model as follows: $K(\mathbf{X}_t, \mathbf{g}_t), (\mathbf{X}_t, \mathbf{g}_t) = \mathbf{K}_t$, $K((\mathbf{X}, \mathbf{g}), (\mathbf{X}, \mathbf{g})) = \mathbf{K}_*$ and $K((\mathbf{X}_t, \mathbf{g}_t), (\mathbf{X}, \mathbf{g})) = \mathbf{K}_{t,*}$, where $\mathbf{g} = (g, \dots, g)^T$ is a vector with length n . It

then follows that these potential outcomes adhere to a multivariate normal distribution, characterized by the mean:

$$\mathbb{E}[f_a(g, X)] = \mathbf{K}_{t,*}^T \cdot [\mathbf{K}_t + \sigma_t^2 \mathbf{I}]^{-1} \cdot \mathbf{y}_t \quad (8)$$

And covariance matrix:

$$\text{Cov}[f_a(g, X)] = \mathbf{K}_* - \mathbf{K}_{t,*}^T \cdot [\mathbf{K}_t + \sigma_t^2 \mathbf{I}]^{-1} \cdot \mathbf{K}_{t,*} \quad (9)$$

Following the definitions of overall treatment effects function and spillover effects function, their estimators can be shown as follows,

$$\hat{\tau}_1(g) = \hat{m}_1(g) - \mathbb{E}[\hat{m}_0(0)] \quad (10)$$

$$\hat{\tau}_0(g) = \hat{m}_0(g) - \mathbb{E}[\hat{m}_0(0)] \quad (11)$$

The linear combination of multivariate normal distributions still follows a normal distribution. Therefore, we have,

$$\begin{aligned} \hat{\tau}_1(g) &\sim N(\mathbb{E}[\hat{m}_1(g)] - \mathbb{E}[\hat{m}_0(g)], \text{Var}[\hat{m}_1(g)]) \\ &\sim N\left(\frac{1}{n}(\mathbb{E}[f_1(g, X)] - \mathbb{E}[f_0(0, X)]), \frac{1}{n^2}(\mathbf{e}^T \Sigma [f_1(g, X)] \mathbf{e})\right) \end{aligned} \quad (12)$$

$$\begin{aligned} \hat{\tau}_0(g) &\sim N(\mathbb{E}[\hat{m}_0(g)] - \mathbb{E}[\hat{m}_0(g)], \text{Var}[\hat{m}_0(g)]) \\ &\sim N\left(\frac{1}{n}(\mathbb{E}[f_0(g, X)] - \mathbb{E}[f_0(0, X)]), \frac{1}{n^2}(\mathbf{e}^T \Sigma [f_0(g, X)] \mathbf{e})\right) \end{aligned} \quad (13)$$

3.2 Active Learning with Optimal Assignments

To improve the estimation accuracies, we can iteratively update the experimental design. Our iteration is consist of two steps. The first step identifies the the experimental condition (a^*, g^*) based on existing estimation. It is expected that additional samples with this setting will improve the overall treatment effects. In the second step, given the target (a^*, g^*) , we choose appropriate networks and optimize the treatment assignments for subsequent experiment.

3.2.1 The selection of the target. In the initial experiments, conditions $A = 1, G = 1$ and $A = 0, G = 0$ should have been included. For network data, these two scenarios are easily achievable. This can be done by simply setting the treatment for all individuals in the network to either 1 or 0. Consequently, all the data in the current network will satisfy the aforementioned conditions.

The treatment level selection is determined at the location where the variance of the functions $\hat{\tau}_a(g)$ is maximum. Because of the unique feature of Gaussian process, this variance function is analytically available. This can be mathematically defined as:

$$a^*, g^* = \underset{a, g}{\text{argmax}} \text{Var}[\hat{\tau}_a(g)].$$

We want to highlight that in active learning literature, other type of criteria can be used as well. For example, choosing the (a^*, g^*) such that the integrated mean square error of the entire function can be reduced most.

3.2.2 Mapping the pair (a^*, g^*) onto the vector \mathcal{A}^* . Upon the selection of the target condition (a^*, g^*) , it becomes imperative to determine the assignments for subsequent experiments, thereby facilitating the active learning process. This necessitates the allocation of a vector-based treatment \mathcal{A}^* within the network. To enhance the efficacy of the matching method in estimating effects, the mapping from (a^*, g^*) to \mathcal{A}^* aims to achieve two primary objectives: first, it maximizes the volume of data within a small interval surrounding the target (a^*, g^*) , which is $(A = a^*, G \in \mathcal{G}^*)$;

second it maximizes the dispersion of the covariates X within the range $(A = a^*, G \in \mathcal{G}^*)$. ($\mathcal{G}^* = [g^* - \alpha/2, g^* + \alpha/2]$)

In the realm of applications, our sample data often encompass multiple networks or can be easily segmented into multiple networks, each with distinct configurations and sizes. Specifically, we consider a scenario with Q networks. The q -th network, denoted by $N = N_q$, comprises n_q individuals. These heterogeneous networks exhibit distinct structural properties, leading to heterogeneity in the transformation from treatment assignment \mathcal{A}_q to the network interference measure (transformed neighbor treatment) G , as well as in the transformation of covariates within neighboring units. For this network, after being assigned with vector-based treatment \mathcal{A}_q , we have some individuals under treatment with $(A = a^*, G \in \mathcal{G}^*)$. This subset of individuals owns a covariates set $X_q^r(\mathcal{A}_q) = (X_{q,1}^r(\mathcal{A}_q), \dots, X_{q,n_q}^r(\mathcal{A}_q))(\mathcal{A}_q)^T$ with length $n_q^r(\mathcal{A}_q)$. In order to obtain the optimal \mathcal{A}_q^* , we maximize the fitness function for different networks (by using the genetic algorithm in algorithm 2) ([18]),

$$\max_{\mathcal{A}_q \in \mathbb{R}^{n_q}} \sum_{i=1}^{n_q^r(\mathcal{A}_q)} \sum_{j=1}^{n_q^r(\mathcal{A}_q)} d^2(X_{q,i}^r(\mathcal{A}_q), X_{q,j}^r(\mathcal{A}_q)), \quad (14)$$

where $d(X_{q,i}^r(\mathcal{A}_q), X_{q,j}^r(\mathcal{A}_q))$ denotes the distance between these two covariates, which could be the Euclidean distance, the Manhattan distance, or other similar distance measures, to describe dispersion while also relating to the number of samples.

Each network (for example, the q -th network) will obtain an optimal solution \mathcal{A}_q^* , along with the corresponding optimal value F_q^* . The amount of data in the vicinity of the targeted interval around (a^*, g^*) is denoted as $n_q^r(\mathcal{A}_q^*)$. Upon selecting a target (a^*, g^*) , to effectively utilize the matching method, we define the lower bound of data volume for $(A = a^*, G \in \mathcal{G}^*)$ as M .

In summary, algorithm 1 shows the Active Learning Algorithm with initialization $N = \{N_1, \dots, N_Q\}$, and the dataset $D = \{X, A, G, Y\}$, which initially starts as a set containing only the data of covariates, with other elements being empty. Note, in algorithm 1, $D|_{(A=a^*, G \in \mathcal{G}^*)}$ denotes the subset of data entries in D that have been experimented with and stored, satisfying the conditions $(A = a^*, G \in \mathcal{G}^*)$. The notation $|D|_{(A=a^*, G \in \mathcal{G}^*)}$ denotes the number of such entries.

4 EXPERIMENTAL RESULTS

4.1 Simulation Data Experiment

Our simulation experiments utilized 100 networks, each contains 100 individuals with three features. Among these, X_1 is a binary variable taking on values of 0 or 1, while the other two, X_2 and X_3 , are continuous variables ranging from 0 to 1. The actual outcome $Y_i(a, g)$ for each individual under the treatment level (a, g) is given by:

$$\begin{aligned} Y_i(a, g) &= (\beta_{1,1} \cdot C_{1,i}^2 + \beta_{1,2} \cdot C_{2,i} + \beta_{1,3} \cdot \frac{1}{C_{3,i} + 1}) \cdot a \\ &+ (\beta_{0,1} \cdot C_{1,i}^2 + \beta_{0,2} \cdot C_{2,i} + \beta_{0,3} \cdot \frac{1}{C_{3,i} + 1}) \cdot (1 - a) \\ &+ \left((\beta_{1,1}^N \cdot (C_{1,i}^N)^2 + \beta_{1,2}^N \cdot \frac{1}{1 + C_{2,i}^N} + \beta_{1,3}^N \cdot C_{3,i}^N) \cdot g \right. \\ &\left. + (\beta_{0,1}^N \cdot (C_{1,i}^N)^2 + \beta_{0,2}^N \cdot \frac{1}{1 + C_{2,i}^N} + \beta_{0,3}^N \cdot C_{3,i}^N) \cdot (1 - g) \right) \\ &\cdot (g - 0.5) + \varepsilon_i, \end{aligned} \quad (15)$$

Algorithm 1 Active learning Algorithm Description

Input networks N and dataset D , lower bound M , empty points set E , using treatment levels number upper limit T
 Get initial targeted treatment level (a^*, g^*)
for i in T **do**
 for N_q in N **do**
 Get $\mathcal{A}_q^*, F_q^*, m_q^*$ by fitting the formula eq. (14) under targeted treatment level (a^*, g^*)
 if $n_q^r(\mathcal{A}_q^*) \geq M - |D|_{(A=a^*, G \in \mathcal{G})}$ **then**
 $N = N \setminus N_q$
 Do the treatment assignment \mathcal{A}_q^* on N_q , and add data to D
 end if
end for
if $n_q^r(\mathcal{A}_q^*)$ for all N_q in N is smaller than $M - |D|_{(A=a^*, G \in \mathcal{G})}$ **then**
 Sort F^* for all networks decreasingly. Get rank R
 Get k with $\sum_{i=1}^{k-1} F_{R^{-1}(i)}^* < M - |D|_{(A=a^*, G \in \mathcal{G})}$ and $\sum_{i=1}^k F_{R^{-1}(i)}^* \geq M - |D|_{(A=a^*, G \in \mathcal{G})}$
 Assign treatment $\{\mathcal{A}_{R^{-1}(1)}^*, \dots, \mathcal{A}_{R^{-1}(k)}^*\}$ onto $\{N_{R^{-1}(1)}, \dots, N_{R^{-1}(k)}\}$, and add data to D
 $N = N \setminus \{N_{R^{-1}(1)}, \dots, N_{R^{-1}(k)}\}$
end if
 Add (a^*, g^*) to E
 Do Gaussian Process Regression to get average overall treatment effect functions and average spillover effect functions
 Select new (a^*, g^*)
end for

where the neighborhood averages $X_{k,i}^N$ for $k = 1, 2, 3$ are defined as:

$$C_{k,i}^N = \frac{\sum_{j=1}^n w_{ij} \cdot C_{k,j}}{\sum_{j=1}^n w_{ij}}, \quad k = 1, 2, 3. \quad (16)$$

Based on our active learning framework applied to this simulation data, we obtained the results shown in Figure 5. Note that after initializing the calculations for the points $(0, 0)$ and $(1, 1)$, our next choice of points was $(0, 0.5)$ and $(1, 0.5)$. This intuitive selection aids in our initial Gaussian process regression, after which we adopt a treatment level selection method based on maximum uncertainty.

We observe that in Figure 5(d), we have achieved considerably good regression results for both overall treatment effects function and spillover effects function. At this point, we have only used 9 networks, conducting experiments on a total of 100×9 individuals. This number is significantly less than the $100 \times 100 = 10,000$ individuals in the complete dataset. In essence, our method has enabled us to make accurate estimates of the average effects for 10,000 individuals using only a limited number of experiments.

The simple random treatment allocation (RTA) is applied for comparison. It first randomly selects the g^* for subsequent experiments, and then it also randomly generates the vector-based treatments allocation based on g^* , as detailed in Appendix A.4. From the simulation comparisons, the proposed ACI method surpass those of

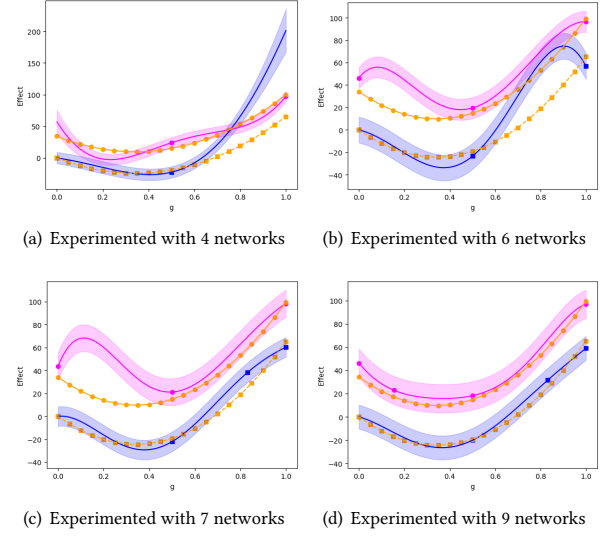


Figure 5: Active Learning in Causal Inference with Interference (ACI) method: The light pink and dark blue curves represent the estimated average overall and spillover effects, respectively. Points along these curves represent sequentially selected treatment levels. It should be noted that there may be instances where two updates occur simultaneously, yet not all are depicted graphically; for example, transitioning from subfigure (a) to (b) introduces two additional sequential treatment levels. The actual scenarios of these effects are shown by two orange dashed curves.

the RTA method. Moreover, the ACI method demonstrates a process where a function is sequentially optimized in a data-driven manner. Although the RTA's predicted functions also show improvement, they reach a certain limit, making it challenging to fit good functions perfectly across the entire range.

Additionally, the Estimated Integral Square Errors (EISE), defined below,

$$EISE(\hat{\tau}_1) = \int (\hat{\tau}_1(g) - \tau_1(g))^2 dg$$

$$EISE(\hat{\tau}_0) = \int (\hat{\tau}_0(g) - \tau_0(g))^2 dg$$

for two different average effects functions at different stages are presented in Table 1.

These superiorities of the ACI method can be attributed to two main reasons: (i) the RTA method lacks a data-driven selection of the optimal treatment level for the next experiment based on existing experimental results; (ii) RTA does not utilize an optimization algorithm to map the target treatment level to an optimal vector-based treatment level, making it challenging to capture the data characteristics at this target treatment level fully.

Moreover, it is important to emphasize that RTA essentially employs the GPR method. Although it cannot guarantee optimal data selection in the active learning phase, as can be observed in Figure 6(d), the predicted functions remain accurate within certain ranges where data is readily available. This further illustrates the

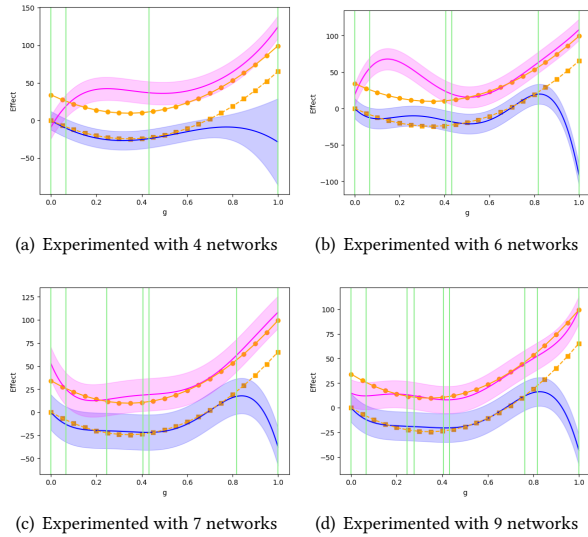


Figure 6: Comparative random treatment allocation (RTA) method: The light pink and dark blue curves illustrate the regression-derived average overall treatment effect and spillover effect. The light green vertical lines represent the position of the randomly selected g^* .

Table 1: Comparison of EISE for ACI and RTA

Experimented networks' number	Effect functions	EISE	
		ACI	RTA
4	$\tau_1(g)$	85.39438557	447.59047721
	$\tau_0(g)$	1814.645103	765.83402693
6	$\tau_1(g)$	338.79261773	565.92932241
	$\tau_0(g)$	395.465169	968.10501448
7	$\tau_1(g)$	592.60175094	34.5195497
	$\tau_0(g)$	51.28109163	443.99716071
9	$\tau_1(g)$	31.74120205	39.42437691
	$\tau_0(g)$	14.60991894	517.14218562

advantage of our GPR method. However, to elaborate further, Figure 6 achieves better results within a certain range largely due to good fortune. Given that our experiments are conducted on a network-level basis, the number of individuals involved in each experiment correlates with the size of the network. This leads to the possibility, under the RTA method, of obtaining a significant amount of data at various treatment levels due to favorable circumstances. Yet, even under these conditions, its results are still inferior to ACI's. Not to mention that, in reality, we might be able to use graph theory knowledge to delineate smaller yet reasonable networks for experimentation.

4.2 Real Data Experiment

Working in partnership with Tencent, we conducted a practical evaluation of our proposed methodology using data from an online

experiment on a mobile game. This gaming experiment aimed to ascertain whether or not a treatment led to increased player engagement compared to the control group. Engagement was measured, for example, by the average online time of the user population. Our analysis investigated the effects of own treatment A and integrated neighbors' treatment G on the average online time across the user community. We established relational networks among the participants, considering in-game social connections, and included both the number of friends and the KDA ratio (Kill, Death, Assist ratio, a common indicator of gaming proficiency) as key covariates. Employing an active learning approach in conjunction with Gaussian Process regression, we achieved significant results with the estimated effects functions. As depicted in Figure 7, we successfully predicted the overall potential outcomes function and the spillover potential outcomes function, using experimental data from 33523 individuals among the entire population of 125286 individuals.

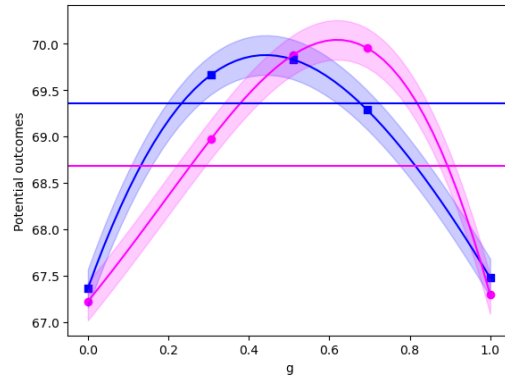


Figure 7: The case study's implementation of the Active Learning in Causal Inference with Interference (ACI) method: The light pink and dark blue functions represent the estimated average overall and spillover potential outcomes, respectively. Points along these curves represent sequentially selected treatment levels. The horizontal lines in light pink and dark blue, respectively, signify the predicted potential outcomes under treatment and control conditions, excluding the consideration of interference.

As shown in Figure 7, the results indicated that both the overall treatment effects function and the spillover effects function increase at the beginning and then decrease after reaching the maximum. This aligns with psychological patterns observed in gaming, where having a few treated friends might encourage one's increased engagement in the game. However, if too many friends receive treatment, it can lead to a decrease in an individual's effect due to a lack of perceived exclusivity or feelings of jealousy. Moreover, we observe the peak of the overall treatment effects occurs to the right of the spillover effects, suggesting that individuals who are treated themselves are more tolerant of a larger proportion of their friends being treated. Additionally, the small difference between the overall treatment effect and spillover effect at the endpoints when $G = 0$ or $G = 1$ reflects that when all or none of an individual's friends are

treated, the individual's own treatment has minimal effects. This is consistent with the inherent social nature of the game.

Based on the results, we identified the treatment level that yields the maximum effect ($A = 1, G = 0.612$). However, it is not feasible to allocate everyone in the population to this treatment level ($A = 1, G = 0.612$). While determining the optimal decision-making strategy based on the estimated functions is not the primary focus of this paper, the results roughly suggest that treating about 50% of the individuals in the population could potentially achieve the optimal average treatment effect.

Additionally, we conducted an analysis under the assumption of ignoring interference. This resulted in two horizontal lines in fig. 7. We found that the average treatment effect, while ignoring interference, is a negative value, -0.673 . In contrast, when considering interference, the optimal average treatment effect at ($A = 1, G = 0.612$) is a positive value, 2.681 . This indicates that ignoring interference in the analysis could mislead decision-making, suggesting a complete rejection of the treatment, which is not the case in reality. This discrepancy arises because the distribution of G in the population used for the experiment tends to favor smaller values, where the direct treatment effects are negative, leading to a negative average treatment effect when interference is ignored. This underscores the necessity and advantage of considering interference, as emphasized by our proposed method.

5 CONCLUSION

We propose a novel active learning approach that enables data-driven experimental design, facilitating causal research and estimation of treatment effects in extensive network data with interference, using minimal data. Our method, validated through simulation experiments, demonstrates the feasibility of obtaining accurate effects estimation with reduced data requirements, significantly enhancing data efficiency. Additionally, a real-world data application has confirmed our approach's practical usability and value in actual business contexts.

Looking forward, potential innovations could involve increasing network complexity beyond the static network structures used in this paper. In real-world settings, dynamic network structures are common, where relationships might exist only temporarily, and individuals might have different neighborhoods at varying times. Moreover, the current methodology for integrating neighbors' covariates and treatments may not be the most effective way to extract information from neighborhoods. Advanced techniques like neural networks or other dimensionality reduction methods might be more efficient to extract information from neighborhoods. Moreover, regarding the current method of integrating neighbors' treatments, within a network, the states ($a = 0, g = 0$) and ($a = 1, g = 1$) are easily achievable. However, reaching states like ($a = 0, g = 1$) and ($a = 1, g = 0$) can be challenging. If a sufficient number of these two types of data is required, extensive experimentation across multiple networks may be necessary. Perhaps a method could be developed, for instance, by using the easily attainable states ($a = 0, g = 0$) and ($a = 1, g = 1$), or by combining other readily available treatment level scenarios. This could enable the estimation of outcomes under challenging treatment levels like

($a = 0, g = 1$) and ($a = 1, g = 0$) without the need for direct experimentation in these hard-to-achieve conditions. Furthermore, guided by our estimated functions, decision-making can be informed to potentially determine what percentage of individuals in the population should be treated, or to devise an optimal vector-based treatment assignment for a group within a network.

REFERENCES

- [1] Alberto Abadie and Guido Imbens. 2002. Simple and bias-corrected matching estimators for average treatment effects.
- [2] Alberto Abadie and Guido W Imbens. 2011. Bias-corrected matching estimators for average treatment effects. *Journal of Business & Economic Statistics* 29, 1 (2011), 1–11.
- [3] Peter M Aronow and Cyrus Samii. 2017. Estimating average causal effects under general interference, with application to a social network experiment. (2017).
- [4] Sarah Baird, J Aislinn Bohren, Craig McIntosh, and Berk Ozler. 2014. Designing experiments to measure spillover effects. (2014).
- [5] Jake Bowers, Mark M Fredrickson, and Costas Panagopoulos. 2013. Reasoning about interference between units: A general framework. *Political Analysis* 21, 1 (2013), 97–124.
- [6] Victor Chernozhukov, Denis Chetverikov, Mert Demirer, Esther Duflo, Christian Hansen, Whitney Newey, and James Robins. 2018. Double/debiased machine learning for treatment and structural parameters.
- [7] David Roxbee Cox. 1958. Planning of experiments. (1958).
- [8] Dean Eckles, René F Kizilcec, and Eytan Bakshy. 2016. Estimating peer effects in networks with peer encouragement designs. *Proceedings of the National Academy of Sciences* 113, 27 (2016), 7316–7322.
- [9] Laura Forastiere, Edoardo M Airolidi, and Fabrizia Mealli. 2021. Identification and estimation of treatment and interference effects in observational studies on networks. *J. Amer. Statist. Assoc.* 116, 534 (2021), 901–918.
- [10] Laura Forastiere, Fabrizia Mealli, Albert Wu, and Edoardo M Airolidi. 2022. Estimating causal effects under network interference with Bayesian generalized propensity scores. *The Journal of Machine Learning Research* 23, 1 (2022), 13101–13161.
- [11] Bryan S Graham, Guido W Imbens, and Geert Ridder. 2010. *Measuring the effects of segregation in the presence of social spillovers: a nonparametric approach*. Technical Report. National Bureau of Economic Research.
- [12] M Elizabeth Halloran and Claudio J Struchiner. 1991. Study designs for dependent happenings. *Epidemiology* 2, 5 (1991), 331–338.
- [13] M Elizabeth Halloran and Claudio J Struchiner. 1995. Causal inference in infectious diseases. *Epidemiology* (1995), 142–151.
- [14] Miguel A Hernán and James M Robins. 2010. Causal inference.
- [15] Guanglei Hong and Stephen W Raudenbush. 2006. Evaluating kindergarten retention policy: A case study of causal inference for multilevel observational data. *J. Amer. Statist. Assoc.* 101, 475 (2006), 901–910.
- [16] Yiyan Huang, Cheuk Hang Leung, Qi Wu, Xing Yan, Shumin Ma, Zhiri Yuan, Dongdong Wang, and Zhixiang Huang. 2022. Robust causal learning for the estimation of average treatment effects. In *2022 International Joint Conference on Neural Networks (IJCNN)*. IEEE, 1–9.
- [17] Michael G Hudgens and M Elizabeth Halloran. 2008. Toward causal inference with interference. *J. Amer. Statist. Assoc.* 103, 482 (2008), 832–842.
- [18] Adam Kolacz and Przemysław Grzegorzewski. 2016. Measures of dispersion for multidimensional data. *European Journal of Operational Research* 251, 3 (2016), 930–937.
- [19] Michael P Leung and Pantelis Loupos. 2022. Unconfoundedness with network interference. *arXiv preprint arXiv:2211.07823* (2022).
- [20] Fan Li, Kari Lock Morgan, and Alan M Zaslavsky. 2018. Balancing covariates via propensity score weighting. *J. Amer. Statist. Assoc.* 113, 521 (2018), 390–400.
- [21] Lan Liu, Michael G Hudgens, and Sylvia Becker-Dreps. 2016. On inverse probability-weighted estimators in the presence of interference. *Biometrika* 103, 4 (2016), 829–842.
- [22] Xinwei Ma and Jingshen Wang. 2020. Robust inference using inverse probability weighting. *J. Amer. Statist. Assoc.* 115, 532 (2020), 1851–1860.
- [23] Elizabeth L Ogburn, Oleg Sofrygin, Ivan Diaz, and Mark J Van der Laan. 2022. Causal inference for social network data. *J. Amer. Statist. Assoc.* (2022), 1–15.
- [24] Elizabeth L Ogburn and Tyler J VanderWeele. 2014. Causal diagrams for interference. (2014).
- [25] Carl Edward Rasmussen, Christopher KI Williams, et al. 2006. *Gaussian processes for machine learning*. Vol. 1. Springer.
- [26] James M Robins, Andrea Rotnitzky, and Lue Ping Zhao. 1994. Estimation of regression coefficients when some regressors are not always observed. *Journal of the American statistical Association* 89, 427 (1994), 846–866.
- [27] Paul R Rosenbaum. 2007. Interference between units in randomized experiments. *Journal of the American statistical association* 102, 477 (2007), 191–200.

- [28] Paul R Rosenbaum and Donald B Rubin. 1983. The central role of the propensity score in observational studies for causal effects. *Biometrika* 70, 1 (1983), 41–55.
- [29] Donald B Rubin. 1974. Estimating causal effects of treatments in randomized and nonrandomized studies. *Journal of educational Psychology* 66, 5 (1974), 688.
- [30] Donald B Rubin. 1980. Randomization analysis of experimental data: The Fisher randomization test comment. *Journal of the American statistical association* 75, 371 (1980), 591–593.
- [31] Eric Schulz, Maarten Speekenbrink, and Andreas Krause. 2018. A tutorial on Gaussian process regression: Modelling, exploring, and exploiting functions. *Journal of Mathematical Psychology* 85 (2018), 1–16.
- [32] Eli Sherman and Ilya Shpitser. 2018. Identification and estimation of causal effects from dependent data. *Advances in neural information processing systems* 31 (2018).
- [33] Michael E Sobel. 2006. What do randomized studies of housing mobility demonstrate? Causal inference in the face of interference. *J. Amer. Statist. Assoc.* 101, 476 (2006), 1398–1407.
- [34] Eric J Tchetgen Tchetgen and Tyler J VanderWeele. 2012. On causal inference in the presence of interference. *Statistical methods in medical research* 21, 1 (2012), 55–75.
- [35] Mark J Van der Laan. 2014. Causal inference for a population of causally connected units. *Journal of Causal Inference* 2, 1 (2014), 13–74.
- [36] Tyler J VanderWeele, Guanglei Hong, Stephanie M Jones, and Joshua L Brown. 2013. Mediation and spillover effects in group-randomized trials: a case study of the 4Rs educational intervention. *J. Amer. Statist. Assoc.* 108, 502 (2013), 469–482.
- [37] Francesco Vivarelli and Christopher Williams. 1998. Discovering hidden features with Gaussian processes regression. *Advances in Neural Information Processing Systems* 11 (1998).
- [38] Shu Yang and Yunshu Zhang. 2023. Multiply robust matching estimators of average and quantile treatment effects. *Scandinavian Journal of Statistics* 50, 1 (2023), 235–265.

A APPENDIX

A.1 Combined kernel function

In order to perform Gaussian Process Regression (GPR), we need to define our kernel to represent the correlation between two data points. In our GPR problem, the features are of two types: one is the integrated neighbors’ treatment G , and the other is the integrated covariates X . In the causal structure, these two types of variables have distinct properties; hence, they should not be considered equivalent in the kernel. For instance, the kernel function is employed to model the influence of neighbors’ treatments and the interaction between this treatment and covariates on the potential outcome ([25]),

$$k((x, g), (x', g')) = k_g(g, g') + \sum_{j=1}^p k_j((x_j, g), (x'_j, g')) \quad (17)$$

Alternatively, with a primary focus on scenarios where the covariates X are high-dimensional, and recognizing that different types of covariates exert anisotropic effects on the outcome, we have developed a specific kernel to tackle this issue. This kernel is intentionally designed to mirror the distinct causal relationships between G and X , and to effectively capture the anisotropic nature inherent within X ,

$$k((x, g), (x', g')) = \sigma_x^2 \exp\left(-\frac{1}{2}(x - x')^T Q (x - x')\right) + \sigma_g^2 \exp\left(-\frac{1}{2\lambda_g^2}(g - g')^2\right) \quad (18)$$

Where Q is a positive definite, diagonal matrix, borrowing idea from [25] and [37].

A.2 Optimizing hyper-parameters

To optimize the hyperparameters such as the length-scale and signal variance in Gaussian Process Regression (GPR), one typically maximizes the marginal (log) likelihood function of the training data ([25, 31]).

Given a set of training data and hyper-parameters denoted as θ , the log marginal likelihood is expressed as:

$$\log p(\mathbf{y}_t | X, \mathbf{g}, \theta) = -\frac{1}{2} \mathbf{y}_t^T [\mathbf{K}_t + \sigma_t^2 \mathbf{I}]^{-1} \mathbf{y}_t - \frac{1}{2} \log |\mathbf{K}_t + \sigma_t^2 \mathbf{I}| - \frac{n_t}{2} \log 2\pi$$

To utilize gradient descent methods such as Standard Gradient Descent, Conjugate Gradient Descent, and Limited-memory Broyden–Fletcher–Goldfarb–Shanno Algorithm, it’s necessary to calculate the partial derivatives of the log likelihood function Equation A.2 with respect to the hyper-parameters θ . The derivative can be expressed as:

$$\begin{aligned} \frac{\partial \log p(\mathbf{y}_t | X, \mathbf{g}, \theta)}{\partial \theta_j} &= \frac{1}{2} \mathbf{y}_t^T [\mathbf{K}_t + \sigma_t^2 \mathbf{I}]^{-1} \mathbf{y}_t \\ &\quad - \frac{1}{2} \text{tr} \left([\mathbf{K}_t + \sigma_t^2 \mathbf{I}]^{-1} \frac{\partial [\mathbf{K}_t + \sigma_t^2 \mathbf{I}]}{\partial \theta_j} \right) \\ &= \frac{1}{2} \text{tr} \left(\left(\boldsymbol{\alpha} \boldsymbol{\alpha}^T - [\mathbf{K}_t + \sigma_t^2 \mathbf{I}]^{-1} \right) \frac{\partial [\mathbf{K}_t + \sigma_t^2 \mathbf{I}]}{\partial \theta_j} \right) \end{aligned}$$

with $\boldsymbol{\alpha} = [\mathbf{K}_t + \sigma_t^2 \mathbf{I}]^{-1} \mathbf{y}_t$.

A.3 Genetic Algorithm

The algorithm 2 presents a simplified version of the genetic algorithm used in our computations. In practice, to prevent overfitting, an early stopping criterion is implemented, which terminates the algorithm if there is no improvement in the fitness value within a certain number of generations. Additionally, the initialization function, roulette-wheel selection function, and crossover mutation function utilized within the algorithm have been specifically tailored to address our particular problem set.

A.4 Random treatment allocation

Similar to the proposed method, the random treatment allocation also initiates with base points $A = 1, G = 1$ and $A = 0, G = 0$. Then, the selection process alternates between points with $A = 1$ and $A = 0$, striving for a balance in representation. However, we decide g^* randomly from a uniform distribution over the interval $(0, 1)$, denoted as $g^* \sim \mathcal{U}(0, 1)$. After determining g^* , to ensure comparability with the guidelines of the proposed method, it is necessary to ensure that the simulation of the random treatment allocation method uses the same number of networks as the proposed method. Assume that the proposed method uses N_u networks and predicts effect values for n_u (A, G) point pairs. The number of networks used for treatment assignments in the random treatment allocation can be represented as N_r , a vector of length n_u , as seen in Algorithm 3. Subsequently, for nodes of selected networks, we assign $A = 1$ to a proportion of nodes as determined by g^* .

Algorithm 2 Optimization for Current Network

Input: target neighbors' treatment g , target's own treatment a , blocking length α , relation matrix W , number of epochs epoch, parameter k , number of batches per epoch K
Initialize the initial set of K parents \mathcal{A}^K
for each epoch i **do**
 Calculate fitness value F^K for the K parent vector-based treatments \mathcal{A}^K using eq. (14)
 for i in K **do**
 Select two parents from the K parents using a roulette-wheel selection method
 Generate two children by crossover of the two selected parents, and calculate the fitness value for each child using eq. (14); select the child with the higher fitness value
 Store this selected child in \mathcal{A}_C^K
 end for
 From \mathcal{A}^K and \mathcal{A}_C^K , select K treatments with the higher fitness value to update \mathcal{A}^K
end for
return The best treatment assignment is the one in \mathcal{A}^K with the highest fitness value

Algorithm 3 Even Distribution of an Integer

Require: Integer N_u , number of parts n_u
Ensure: Vector \mathbf{N}_r of length n_u with distributed values
 $base \leftarrow \lfloor N_u/n_u \rfloor$
 $remainder \leftarrow N_u \bmod n_u$
 Initialize vector $\mathbf{N}_r[1 \dots n_u]$ to $base$
 for $i = 1$ to $remainder$ **do**
 $\mathbf{N}_r[i] \leftarrow \mathbf{N}_r[i] + 1$
 end for
return \mathbf{N}_r
